Catalysis Science & Technology

Accepted Manuscript

ROYAL SOCIETY OF CHEMISTRY

www.rsc.org/catalysis

Journal Name

ARTICLE

Stability, Scalability, and Reusability of a Volume Efficient Biocatalytic System Constructed on Magnetic Nanoparticles

Gayan Premaratne,[a] Rajasekhara Nerimetla,[a] Ryan Matlock,[a] Loren Sunday,[a] Rangika S. Hikkaduwa Koralege,[b] Joshua D. Ramsey,[b] and Sadagopan Krishnan[a,*]

Received 00th January 20xx,
Accepted 00th January 20xx

DOI: 10.1039/x0xx00000x

www.rsc.org/

This report investigates for the first time stability, scalability, and reusability characteristics of a protein nano-bioreactor useful for green synthesis of fine chemicals in aqueous medium extracting maximum enzyme efficiency. Enzyme catalysts conjugated with magnetic nanomaterials allow easy product isolation after a reaction involving simple application of a magnetic field. In this study, we examined a biocatalytic system made of peroxidase-like myoglobin (Mb), as a model protein, to covalently conjugate with poly(acrylic acid) functionalized magnetic nanoparticles (MNPs, 100 nm hydrodynamic diameter) to examine the catalytic stability, scalability, and reusability features of this bioconjugate. Application of the conjugate was effective for electrochemical reduction of organic and inorganic peroxides, and for both peroxide-mediated and electrocatalytic oxidation of the protein substrate 2, 2'-azino-bis(3-ethylbenzothiazoline-6-sulfonic acid) with greater turnover rates and product yields than Mb prepared in solution or MNP alone. Mb-attached MNPs displayed extensive catalytic stability even after 4 months of storage compared to Mb present in solution. Five- and ten-fold scale up of MNPs in the bioconjugates resulted in two- and four-fold increases in protein-catalyzed oxidation products, respectively. Nearly 40% of the initial product was present even after four reuses, which is advantageous for synthesizing sufficient products with a minimal investment of precious enzymes. Thus, the results obtained in this study are highly significant in guiding cost-effective development and efficient multiple uses of enzyme catalysts for biocatalytic, electrocatalytic, and biosensing applications via magnetic nanomaterials conjugation.

Introduction

Volume efficient, stable, scalable, and reusable enzymatic bioreactors are crucial for cost-effective green stereoselective synthesis of fine chemicals and specialty materials and for niche biosensing applications. In this regard, magnetic nanoparticles (MNPs) are very attractive for a broad range of chemical and biological applications such as separation and purification of biomolecules, imaging, drug delivery, catalysis, cancer therapy, design of bioelectrodes, and sensitive biosensors.[1-12] MNPs offer a large specific surface area and can be equipped with desired chemical functional groups for covalent conjugation with biomolecules (e.g., proteins, DNA, polymers) and small molecules.[9, 13]

Recently, the enzyme β-glucosidase was cross-linked with super-paramagnetic Fe_3O_4 nanoparticles (NPs) using glutaraldehyde reagent.[14] The immobilized enzyme functioned well at an optimum pH of 4.0 and temperatures as high as 80 ^{o}C. The enzyme was stable during storage for 6 weeks. NP surface modification in combination with fusion protein technology has been used to develop maltose-modified magnetic support for use in separation, purification, and immobilization of a maltose binding protein by affinity adsorption.[15]

MNPs have also been used in combination with other nanomaterials to enhance efficiency of biosensors. Long-term stable sensors made of single-walled carbon nanotube-coated MNPs have been used to immobilize amyloglucosidase to effectively hydrolyze starch during a biofuel production process.[16] Magnetic clay composites made of MNPs self-assembled on nanoclays have been used as supports for glucoamylase conjugation. The regenerative properties of the magnetic composites in immobilizing new glucoamylase after the loss of activity of initial glucoamylase molecules also have been documented.[17] Lactase conjugated to MNPs has been observed to retain more than 78% of its activity after five cycles of use with minimal structural and functional changes of the enzyme.[18]

MNPs act as an excellent solid support and uniquely allow easy isolation of the prepared conjugates within a few seconds by simple placement of a magnet around the sample tubes. Many other metal or inorganic NPs do not possess this feature. In this study, we, for the first time examined the stability, scalability, and reusability features of a bioreactor made of cost-effective myoglobin (Mb) metalloprotein model covalently attached to poly(acrylic acid)-functionalized MNPs. Mb possesses peroxidase-like activity and reductively cleaves hydrogen peroxide (H_2O_2), leaving one of the oxidizing equivalents in the form of a ferryloxy species (Fe^{IV}=O).[19, 20] The findings of this study possess high significance for the

[a] *Department of Chemistry, Oklahoma State University, Stillwater, OK 74078, USA E-mail. gopan.krishnan@okstate.edu*
[b] *School of Chemical Engineering, Oklahoma State University, Stillwater, OK 74078, USA.*
The manuscript was written through contributions of all authors. All authors have given approval to the final version of the manuscript.

Scheme 1. Preparation of scalable and reusable protein-MNP conjugates for biocatalytic and biosensing applications.

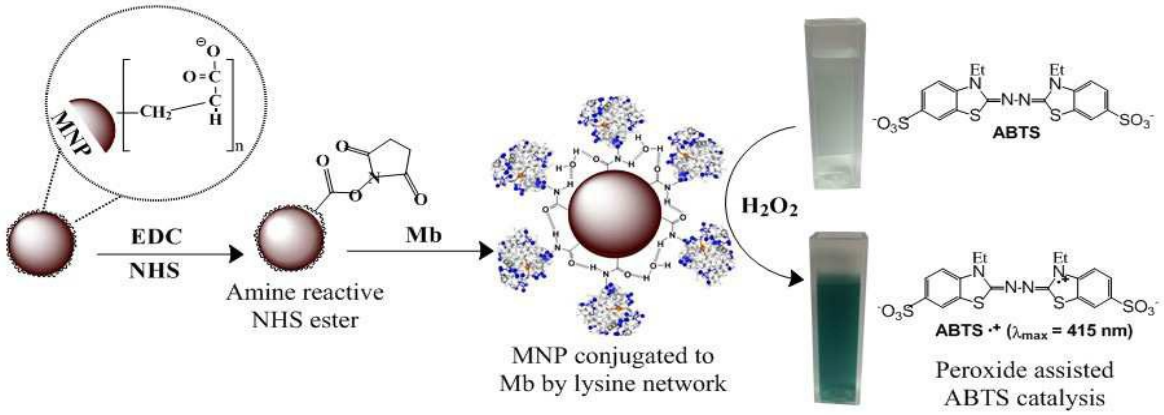

development of cost-effective enzyme-based magnetic nano-bioreactors for stereoselective green synthesis with minimal enzyme use.

Experimental

Chemicals and materials

Poly(acrylic acid)-functionalized magnetic nanoparticles (MNPs, 100 nm hydrodynamic diameter) were purchased from Chemicell GmbH Inc. (Berlin, Germany). Equine heart Mb, H_2O_2, diammonium salt of 2,2′-azino-bis (3-ethylbenzothiazoline-6-sulfonic acid) [ABTS], *tert*-Butyl hydroperoxide (*t*-BuOOH), toluidine blue O (TBO), 1-ethyl-3-[3-dimethylaminopropyl] carbodiimide hydrochloride (EDC), and N-hydroxysuccinimide (NHS) were purchased from Sigma. High purity graphite disk electrodes (HPGs, geometric area 0.2 cm^2) were purchased from McMaster-Carr (Atlanta, GA, USA). All other chemicals were of high purity analytical grade.

Instrumentation

A Varian Cary 100 Bio UV-Vis spectrophotometer was used to identify and quantify the ABTS oxidation product catalyzed by Mb attached to MNPs, the free Mb control, and free MNP control. Fourier transform infrared spectroscopy (FTIR) analysis was conducted for the MNPs, Mb, and Mb-MNPs using a Thermoscientific Nicolet iS50 FTIR. The MNPs and Mb-MNP conjugates were additionally characterized by transmission electron microscopy (TEM, JEOL JEM-2100) by preparing drop coated samples on carbon surfaces of copper grids. The hydrodynamic diameter and surface charges of Mb, MNPs and Mb-MNP conjugates were measured using a ZetaPALS

ζ-potential analyser (Brookhaven Instruments Corporation, Holtsville, NY, USA). A CH 6017E electrochemical analyzer was used to study ABTS oxidation and stability by amperometric i-t curve and peroxide reduction by rotating disc voltammetry.

Immobilization of Mb onto MNPs

The covalent attachment of Mb via its surface lysine residues to the carboxylic acid groups of poly(acrylic acid)-functionalized MNPs followed our previously reported technique.[8] Briefly, freshly prepared aqueous solutions containing EDC (0.35 M) and NHS (0.1 M) were added to 1, 5, and 10 mg of MNPs, and the solutions were incubated for 15 min to activate the carboxylic acid groups of MNPs into easily leaving N-succinimidyl ester units. The free EDC/NHS solution was removed from the activated MNPs by application of a magnetic field. The particles then were washed in phosphate buffer saline (PBS) twice and immediately suspended in a freshly prepared Mb solution (800 µL of 6 mg mL^{-1} in pH 5.0 acetate buffer).

The covalent attachment of Mb to MNPs was carried out for 1 h at room temperature with continuous gentle mixing of the reaction tubes in a tube rotator (Fisher Scientific). Covalently attached Mb-MNP conjugates (Mb-$MNPs_{1mg}$, Mb-$MNPs_{5mg}$, and Mb-$MNPs_{10mg}$) were separated from the free Mb in solution by use of a magnet. The Mb-MNP conjugates were washed twice in PBS, resuspended in a fresh PBS solution (1000 µL), and used for spectral and electrochemical studies. These conjugates were characterized using UV-Vis spectrophotometry, FTIR spectroscopy, DLS studies and TEM.

Oxidation of ABTS catalyzed by Mb-MNP conjugates

To the solutions containing Mb-MNP conjugates (1, 5, or 10 mg MNPs in each conjugate) and ABTS (10 mM), H_2O_2 (1 mM) was added to initiate ABTS oxidation. The reaction was carried out for 10 minutes under constant stirring of the reaction mixture tubes at 100 rpm, at 25 °C. The formation of ABTS radical cation (λ_{max} = 415 nm) in the reaction mixture was monitored using a UV–Vis spectrophotometer (Scheme 1).[21, 22]

After the reaction, the used Mb-MNP conjugates were recovered using a magnet, washed thrice with PBS solution, resuspended in 1 mL of fresh PBS solution, and allowed to stand for 30 min before being used again for a new ABTS reaction. These conjugates were tested for reusability for five times toward ABTS oxidation using the procedure described above. Mb-MNP conjugates also were prepared and stored at 4 °C for 1 week, 2 weeks, and 4 months to assess storage stability towards catalyzing ABTS oxidation. As a representative system, Mb-$MNPs_{1mg}$ was chosen to examine the Michaelis–Menten kinetics of peroxide

assisted ABTS oxidation using varying amounts of H_2O_2 (0.04 – 3.2 mM) and compare with either Mb solution or MNP alone.

Electrochemical conversion of ABTS into its oxidized product was confirmed using chronoamperometry. Prior to use, Mb-MNP conjugates were adsorbed on four polished HPG electrodes kept at 4 °C for 20 min. The electrodes then were washed with deionized water, and the Mb-MNP adsorbed electrodes were immersed in a beaker containing 10 mL buffer (PBS pH 7.4). Amperometry experiments were performed at an applied potential of –0.5 V vs. the Ag/AgCl reference electrode at 25 °C in stirred and atmospheric air conditions. The electrocatalytic stability of the adsorbed films of Mb-MNP conjugates, Mb solution (1 mg mL^{-1}), and MNP solution (1 mg mL^{-1}) was tested for 3 h by monitoring current over time.

The peroxide reduction activity of the conjugates was evaluated by voltammetry in a three electrode system featuring Mb-MNPs coated on HPG working electrodes, an Ag/AgCl reference electrode, and a Pt-wire counter electrode in a PBS solution (pH 7.4) continuously purged with argon. In all experiments, free Mb solutions and free MNP suspensions prepared in PBS were used as controls.

Results and Discussion

Characterization of Mb-MNP covalent conjugates

Fig. 1 shows the FTIR spectra of free MNPs, free Mb, and Mb-MNP conjugates. The characteristic stretching vibration of the Fe-O bond at 581 cm^{-1} was observed in MNPs, and it slightly shifted to 588 cm^{-1} in Mb-MNPs. The strong and broad O-H stretching band of –COOH in MNPs at 3032 cm^{-1} disappeared when conjugated with Mb, and the appearance of new –NH-CO-(amide) bands at 1637 and 1534 cm^{-1} was noted in the Mb-MNP covalent conjugates (Fig. 1c). These amide bond vibrations are in agreement with those observed in free Mb at 1630 and 1525 cm^{-1} (Fig. 1b). The slightly greater vibration frequency of amide bands suggests the effect of conjugation in the amide bond strength in the Mb-MNP conjugates compared to free Mb. Additionally, a new band at 3281 cm^{-1} in the Mb-MNP covalent conjugates is attributed to the N-H stretching in Mb, which can be seen in free Mb at 3274 cm^{-1}. Thus, the FTIR spectra suggest the covalent conjugation of Mb with MNPs via the standard carbodiimide coupling chemistry.

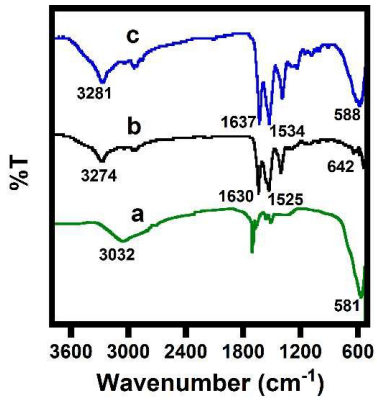

Fig. 1 FTIR spectra of: (a) pure MNPs, (b) pure Mb, and (c) Mb-MNP conjugate.

Toluidine Blue O (TBO) test to estimate the surface -COOH groups of MNPs

The surface poly(acrylic acid)-COOH groups of MNPs were quantitated by a colorimetric assay involving the electrostatic interaction of the negative -COOH groups on MNP surfaces with the cationic TBO dye forming a blue colored solution.[23-25] To minimize any interferences from the surface charges of the magnetite (Fe_3O_4) core of MNPs, we carried out the colorimetric assay in pH 8.0 phosphate buffer, which is the reported isoelectric point for magnetite NPs[26] (i.e., the net surface charge of the magnetite core is zero at pH 8.0, so the major contribution of negative charge is expected to arise from the surface deprotonated –COOH groups of poly(acrylic acid) units). A calibration curve was constructed by using various known concentrations of poly(acrylic acid) standards prepared in phosphate buffer solutions (pH 8.0) and reacted with the TBO reagent under similar conditions (Fig. S1). The absorbance was recorded at 637 nm and the calibration plot was used in determining the surface -COOH concentration of MNPs. The amount of -COOH groups determined from the described assay was 7.1 ± 0.5 ($x10^{17}$) molecules/mg of MNPs. This represents the availability of sufficient number of poly(acrylic acid)-COOH groups in MNPs to covalently conjugate with Mb using the designed carbodiimide chemistry.

Monitoring ABTS oxidation catalyzed by Mb-MNP conjugates

UV-Vis spectrophotometry was used to analyze the spectra arising from pure Mb, MNPs, and the Mb-MNP conjugates. Fig. S2 shows the representative absorbance spectra of free Mb in solution (1 mg mL^{-1}), free MNPs (1 mg mL^{-1}), the Mb-MNP_{1mg} conjugate in PBS solution, and the reaction product of ABTS oxidation catalyzed by the Mb-MNP_{1mg} conjugate. The characteristic Soret band of Mb appeared at 409 nm, and there was little or no Soret band absorbance in the Mb-MNP conjugates. This implies the absence of free Mb in PBS solution and the retention of covalently attached Mb on the surface of MNPs. The Mb Soret absorbance does not interfere with the absorbance of the ABTS oxidation product (415 nm), which thus allows identification and quantification of product yields (Fig. S2). The ABTS oxidation ability by the free MNPs agreed with results of a previously reported study.[22] However, it is to be noted that Mb in solution produced lower product yields than the conjugates (detailed later).

TEM images of MNPs and Mb-MNP conjugates

Figures 2A–D represent the typical TEM images of free MNPs, Mb-$MNPs_{1mg}$, Mb-$MNPs_{5mg}$, and Mb-$MNPs_{10mg}$, respectively. MNPs were nearly spherical in shape and were much smaller than the hydrodynamic 100 nm diameter due to drying and high vacuum conditions applied for TEM imaging (Fig. 2A).[27] Fig. 2B shows a coated layer of Mb around MNPs that is absent in free MNPs, which confirms the attachment of Mb to MNPs. The coated layer of Mb was more prominent with increased amounts of MNPs (Fig. 2B to D), indicating the availability of increasing numbers of –COOH groups of MNPs for greater immobilization of Mb molecules. The

TEM images also show the extended aggregation of Mb-MNP conjugates with increasing MNP amounts, which suggests greater Mb accumulation onto the MNP surface.

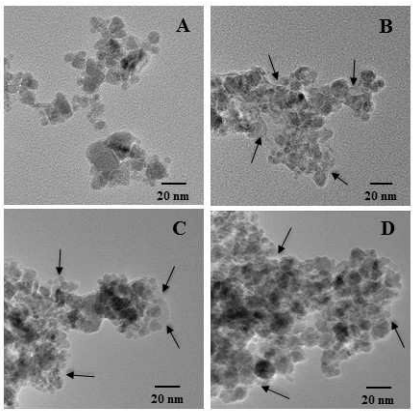

Fig. 2 Typical TEM images of (A) free MNPs, (B) Mb-MNPs$_{1mg}$, (C) Mb-MNPs$_{5mg}$, and (D) Mb-MNPs$_{10mg}$ conjugates. The Mb films around MNPs in each conjugate are indicated by arrow heads.

Hydrodynamic particle size and Zeta potential

The average hydrodynamic particle diameters of MNPs and each conjugate were determined by dynamic light scattering (DLS). Each measurement was taken at a 90° angle for a total of 5 measurements, lasting 2 minutes per measurement. The samples were diluted 50 times prior to measurements in PBS (pH 7.4). Mb with a hydrodynamic diameter of 3.8 nm[28,29] contains 18 surface Lys residues (PDB: 1WLA) for covalent attachment with MNPs. The Mb-MNP conjugates produced larger aggregates (Table 1) with the increment in the amount of MNPs used, which is in agreement with the TEM results presented above. Polydispersity index (PDI) was ≤ 0.2 for the dispersed superparamagnetic MNPs, which is not surprising. However, all three Mb-MNP conjugates also showed PDI ≤ 0.2, which is quite interesting. The observed smaller PDI values suggest that the prepared Mb-MNP conjugates have narrow size distributions.

Table 1. DLS measurements of hydrodynamic diameters (in nm) in PBS (pH 7.4).

	MNPs	Mb-MNPs$_{1mg}$	Mb-MNPs$_{5mg}$	Mb-MNPs$_{10mg}$
Hydrodynamic diameter (nm)	101 ± 2	1226 ± 187	2304 ± 416	4769 ± 626
Polydispersity	0.12 ± 0.01	0.18 ± 0.03	0.18 ± 0.04	0.20 ± 0.013

Phase analysis light scattering (PALS) was used to determine ζ-potentials. The ζ-potential was calculated from the electrophoretic mobility of the particles by employing the Smoluchowski's equation, available with the instrument software. The average ζ-potentials of Mb solution, MNPs alone, and the Mb-MNP conjugates diluted 10 times in PBS (pH 7.4) were calculated from a total of 10 measurements with each measurement lasting 30 seconds (Table 2).

Table 2. The ζ-potentials for the MNPs, Mb, and Mb-MNPs in PBS (pH 7.4).

	MNPs	Mb	Mb-MNPs$_{1mg}$
ζ-potential (mV)	-24 ± 2	-18 ± 1	-13 ± 2

The negative ζ-potential of MNPs is attributed to the negative surface –COOH groups from poly(acrylic acid) functionalization.[30] Similarly, Mb showed a negative ζ-potential due to the net negative charge at pH 7.4 (pI 6.8 and 7.0).[31] Upon covalent attachment of the –COOH activated MNPs with the surface lysine groups of Mb, the complex as a whole displayed a shift in ζ-potential to -13 mV. This could be attributed to the conversion of MNP–COOH groups to amide bonds connecting Mb molecules and the associated decrease in the net negative surface charge of MNPs, and thus suggesting the formation of Mb-MNP conjugate from the carbodiimide-amine coupling reaction.[32,33]

Effect of Mb concentration in the conjugation reaction

We used various amounts of Mb in the MNP conjugation reaction with a constant MNP amount (1, 5, or 10 mg) to determine the amount of protein that would provide maximum binding with MNPs. This factor is controlled by the size of the protein involved and the extent of available surface lysine residues when using amine-coupling with carboxylated MNPs. We determined that a Mb concentration of 6 mg mL^{-1} (800 µL volume, ~ 280 nmoles) provided saturation binding (Fig. 3). Therefore, this concentration was used for conjugation with MNPs to ensure that the amount of Mb present was not a limiting factor when the MNP amount was increased.

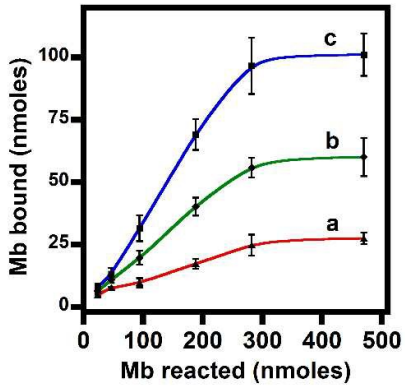

Fig. 3 Plot of bound Mb versus the amount of Mb reacted with (a) 1, (b) 5, or (c) 10 mg of MNPs used in the reaction.

Effect of MNP amount on Mb-MNP conjugates and ABTS oxidation product yields.

Many enzymes are difficult to purify and obtain in large quantities. Hence, it will be advantageous to determine how to make the best catalytic use of a small amount of enzyme upon conjugation with MNPs. For this, we conducted the Mb-MNP conjugation reaction using increasing amounts of EDC/NHS-treated MNPs (1, 5, 10, and 25 mg) with a constant amount of Mb in solution (800 µL volume of 6 mg mL^{-1}). The effect of increasing the amount of MNPs in the conjugation reaction with Mb was examined by measuring the oxidation of ABTS in PBS solution.

Fig. 4 shows that 5 and 10 mg of MNPs increased the amount of ABTS oxidation product by 2- and 4-fold, respectively, relative to 1 mg of MNPs. This suggests that production of product can be scaled up by increasing the amount of MNPs used in conjugate preparation. Moreover, greater product yields were obtained by the Mb-MNP conjugates compared to free Mb and free MNPs at amounts similar to those present in the conjugates. The product yield enhancement is not significantly greater upon using 25 mg of MNPs compared to 10 mg of MNPs to conjugate with Mb (Fig. 4), which indicates that the amounts of Mb used were optimum for the test range of MNP amounts tested. For 1, 5 and 10 mg of MNPs the amount of product catalyzed by the Mb-MNP conjugates was on average 1.5-times greater than that catalyzed by the Mb solution and 5-times greater than that of the MNP solution.

Although, the product enhancement is not significantly greater for Mb-MNP conjugates, there are several unique advantages that are unavailable from free protein solution: the Mb-MNP conjugate retains the protein in the surface-bound form, does not necessitate reactant isolation from products, and does not cause interference from the protein during product analysis after magnetic separation. In contrast, free Mb solution after reaction with ABTS and peroxide cannot be magnetically separated unless analytical separation procedures are used, which require manual labor, time, analysis, and instruments.

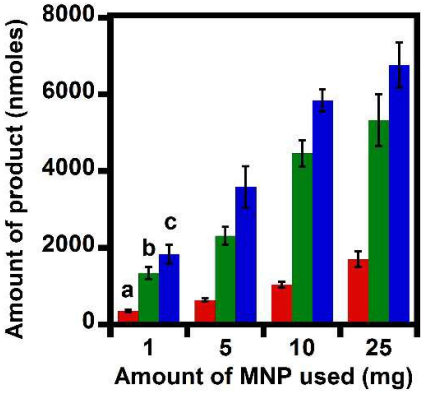

Fig. 4 ABTS oxidation product yields catalyzed by (a) free MNPs, (b) free Mb, and (c) Mb-$MNPs_{1mg}$ conjugates. The corresponding comparative data for samples of Mb-$MNPs_{5mg}$ and Mb-$MNPs_{10mg}$ along with the respective free MNPs and free Mb controls are also shown as labeled in the x-axis. ABTS oxidation was carried out in PBS solution in the presence of hydrogen peroxide (1 mM) at 25 °C, pH 7.4.

Reusability and storage stability are other advantages of the conjugate design as demonstrated below. Thus, the simplicity and enhancement of product yields by the protein-MNP conjugates compared to the free protein reaction are noteworthy in view of broad applications for enzyme catalyzed bioreactors. The intrinsic peroxidase activity of MNPs (Fe_3O_4) may explain their role in the oxidization of ABTS.[22] However, in non-peroxidase reactions, the peroxidase activity of free MNPs may not be significant.

Michaelis-Menten kinetics of peroxide mediated ABTS oxidation

To obtain better insights on the reaction kinetics of MNPs, Mb in solution, and Mb-$MNPs_{1mg}$, we carried out the ABTS oxidation with various concentrations of H_2O_2. The plots of product yield versus the H_2O_2 concentration followed the Michaelis-Menten kinetics (Fig. 5). The kinetic parameters estimated are summarized in Table 3. Mb-$MNPs_{1mg}$ shows comparable affinity to the peroxide as of the free Mb prepared in solution, while the peroxide affinity of only MNPs is relatively smaller. This suggests that MNPs can provide a suitable environment to immobilize enzymes without altering the substrate affinity. Furthermore, the conjugates displayed nearly two fold greater catalytic turnover rate than Mb solution and about 250-fold greater than the MNPs alone (Table 3). The Michaelis-Menten kinetics of electrochemically driven ABTS oxidation by the designed Mb-MNP conjugates and compared with Mb solution or only MNPs are consistent with the results obtained using peroxide-mediated ABTS oxidation (Figures 8 and 9 below for more details).

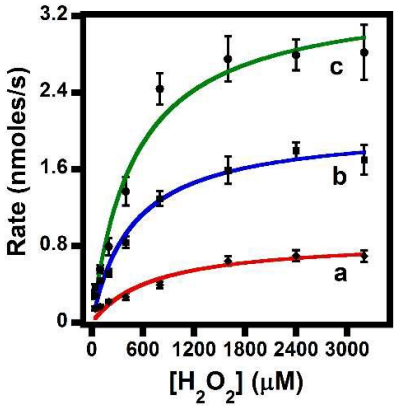

Fig. 5 The Michaelis-Menten kinetics of (a) MNPs, (b) Mb in solution, and (c) Mb-$MNPs_{1mg}$ toward ABTS oxidation under various concentrations of H_2O_2.

Table 3. Kinetic parameters for ABTS oxidation by Mb, MNPs, and Mb-$MNPs_{1mg}$ quantified from the Michaelis-Menten plots.

	MNPs	Mb	Mb-$MNPs_{1mg}$
K_M (µM)	711 ± 121	482 ± 85	504 ± 91
V_{max} (nmoles/s)	0.9 ± 0.1	2.0 ± 0.1	3.4 ± 0.2
K_{cat} (s^{-1})	0.0006 ± 0.21 ($x10^{-4}$)	0.085 ± 0.012	0.153 ± 0.037

Reusability and advantages of Mb-MNP conjugates over free Mb solution

A preferred feature of an effective bioreactor would be reusability for repeated generation of products using only a small amount of enzyme. To assess the reusability of Mb-MNPs, the conjugates were magnetically recovered after each cycle of ABTS oxidation and reused four times by reacting the conjugates with a fresh solution of ABTS and H_2O_2. Fig. 6 shows the amount of ABTS oxidation product formed each time the Mb-MNPs were reused for the conjugates made with 1, 5, and 10 mg of MNPs at the saturating Mb concentration used in the reaction (Fig. 3). About 40% of the initial amount of product was formed after four reuses of the conjugates.

Possible reasons for the decrease in product yield with number of reuses include exposure of the conjugates to repeated peroxide stress and the associated loss in protein activity, possibly caused by the formation of intermediate peroxide radicals during the reaction.[22,34] Furthermore, the conjugates prepared with 10 mg of MNPs produced larger amounts of product after five uses compared to the conjugates made using 1 and 5 mg of MNPs (Fig. 6). The reusability feature of the conjugates is a unique advantage over the free protein solution, which would require additional analytical methods for isolation of protein from the reaction mixture, preconcentration, and characterization steps before reuse in the next batch of reaction.

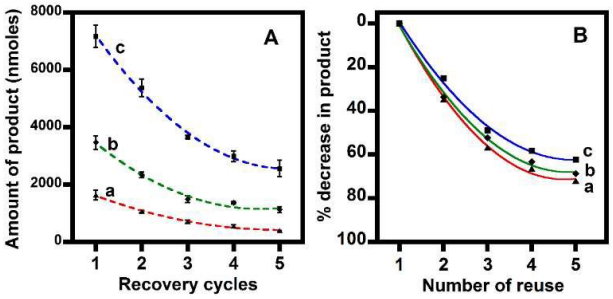

Fig. 6 (A) Amounts of ABTS oxidation product with number of reuses of Mb-MNPs conjugates made of (a) 1, (b) 5, and (c) 10 mg of MNPs. (B) Percentage decrease in amount of product with the number of reuses of the Mb-MNP conjugates.

Storage stability of Mb-MNP conjugates

Storage stability is another important parameter for any bioreactor system. Three Mb-MNP conjugates prepared using varying amounts of MNPs were stored at 4 °C in PBS to assess the effect of storage on protein activity in the ABTS oxidation reaction. About 50% of the initial protein activity was retained in all conjugates even after 4 months of storage. This finding suggests that MNPs act as an excellent support to attach, stabilize, and obtain efficient use of enzymes with good catalytic activity for a reasonably long period of time (Fig. 7).

Electrochemically driven ABTS oxidation by the Mb-MNP conjugates adsorbed on electrodes

The Mb-MNP conjugates were adsorbed on HPG electrodes and tested for the electrochemical conversion of ABTS into oxidation product in atmospheric air in PBS (pH 7.4) under an applied potential of –0.5 V vs. Ag/AgCl to electrochemically reduce Mb heme center to initiate catalysis.

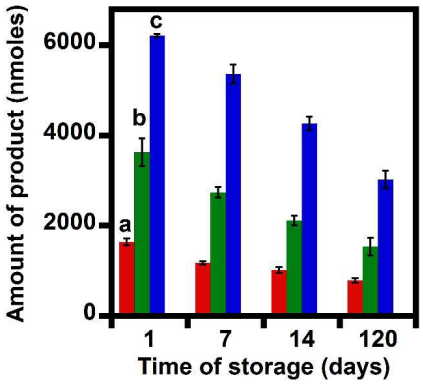

Fig. 7 Storage stability of the Mb-MNP conjugates prepared using (a) 1, (b) 5, and (c) 10 mg of MNPs. Oxidation of 10 mM ABTS in the presence of 1 mM H_2O_2 in PBS solution (pH 7.4), 25 °C was tested on the initial day of the experiment and after 7, 14, and 120 days of storage at 4 °C.

The increments in currents with increasing concentrations of ABTS (35 to 500 μM) were observed (Fig. 8A-C), and the measured currents versus the concentration of ABTS displayed a good fit in the Michaelis-Menten equation (Fig. 8D). The apparent Michaelis-Menten constants (K_m^{app}, in μM) were in the following order: Mb (393 ± 29) ≈ Mb-MNPs$_{1mg}$ (420 ± 50) > Mb-MNPs$_{5mg}$ (235 ± 18) > Mb-MNPs$_{10mg}$ (166 ± 12).

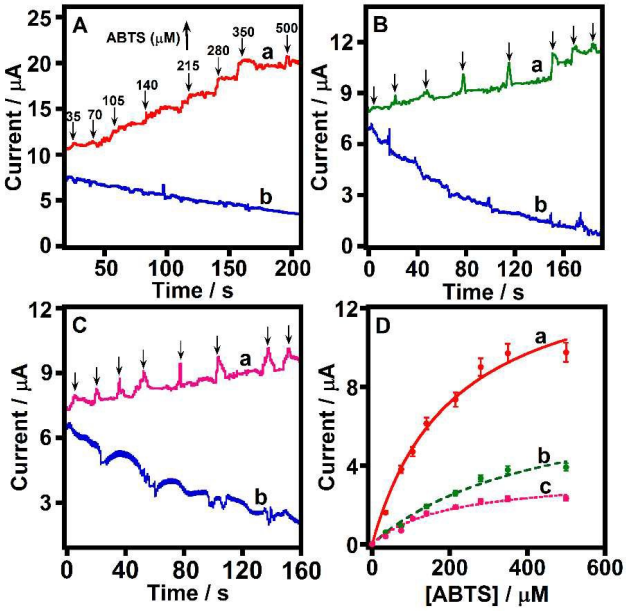

Fig. 8 Amperometric data (i-t curves) for ABTS oxidation by (**A**) (a) HPG/Mb-MNPs$_{10mg}$ and (b) only HPG/MNPs$_{10mg}$ (no Mb control); (**B**) (a) HPG/Mb-MNPs$_{5mg}$ and (b) only HPG/MNPs$_{5mg}$ (no Mb control); and (**C**) (a) HPG/Mb-MNPs$_{1mg}$ and (b) only HPG/MNPs$_{1mg}$ (no Mb control) in PBS, pH 7.4 under saturated atmospheric air conditions at an applied potential of –0.5 V vs. Ag/AgCl, 150 rpm electrode rotation rate, 25 °C. (**D**) Electrochemical

Michaelis-Menten kinetics of ABTS oxidation by (**a**) HPG/Mb-MNPs$_{10mg}$, (**b**) HPG/Mb-MNPs$_{5mg}$, and (**c**) HPG/Mb-MNPs$_{1mg}$ conjugates.

These data suggest greater substrate affinity with increasing amounts of MNPs in the conjugates (i.e., lower K_m^{app}; Figures 8 and 9). Furthermore, the Mb-MNPs conjugates showed better sensing properties for the protein substrate, ABTS, in comparison to free Mb (Fig. 9). The controls (HPG/MNPs$_{10mg}$, HPG/MNPs$_{5mg}$, and HPG/MNPs$_{1mg}$ adsorbed on HPG electrodes) with no Mb showed no increase in currents upon addition of ABTS, which illustrates the role of Mb in catalyzing ABTS electrochemically (Fig. 9) in the presence of atmospheric air. The lack of current increase with free MNP films suggests a lower catalytic efficiency of MNPs in the absence of Mb and the associated poor sensitivity in the amperometry.

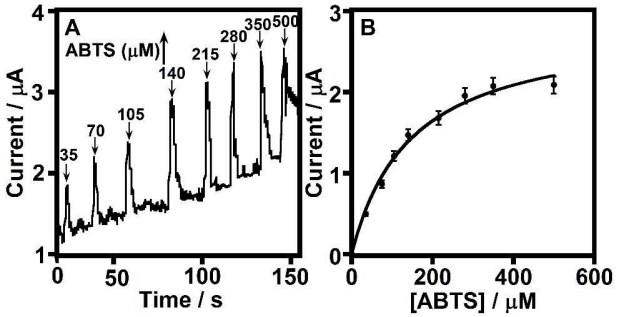

Fig. 9 (**A**) Amperometric data (i-t curve) for ABTS oxidation by HPG/Mb electrodes without MNP conjugation in PBS buffer (pH 7.4) under saturated atmospheric air conditions at an applied potential of –0.5 V vs. Ag/AgCl, 150 rpm rotation rate, 25 ^{o}C. (**B**) Electrochemical Michaelis-Menten kinetics of ABTS electrolysis by HPG/Mb electrodes.

Electrocatalytic oxygen reduction stability studies showed that Mb-MNPs conjugates had better stability on electrodes when greater amounts of MNPs were used in the Mb conjugation reaction in the following order: MNPs < Mb < Mb-MNPs$_{1mg}$ < Mb-MNPs$_{5mg}$ < Mb-MNPs$_{10mg}$ (Fig. 10). The Mb-MNP conjugates retained an average initial oxygen reduction current of about 55% compared to the low residual currents of 38 and 26% in the cases of free Mb and free MNPs films on electrodes, respectively. This suggests better electrostatic and other secondary interactions of the Mb-MNPs conjugates with polished HPG electrodes than for free Mb and free MNPs.

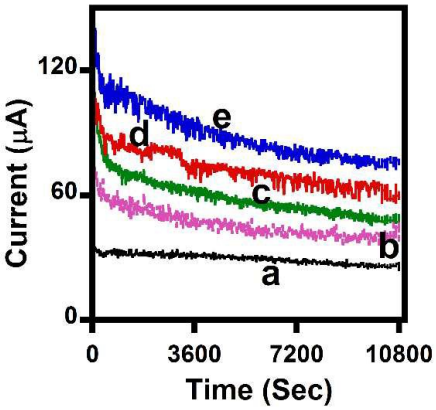

Fig. 10 Electrocatalytic stability (i-t curve) of (**a**) MNPs, (**b**) Mb, (**c**) HPG/Mb-MNPs$_{1mg}$, (**d**) HPG/Mb-MNPs$_{5mg}$, and (**e**) HPG/Mb-MNPs$_{10mg}$ in buffer pH 7.4 PBS under saturated atmospheric air conditions at an applied potential of –0.5 V vs. Ag/AgCl, 150 rpm rotation rate, 25 ^{o}C.

Peroxide catalysis of Mb-MNPs conjugate films coated on electrodes

In addition to the electrochemical substrate biosensing and oxygen reduction applications, we assessed the organic peroxide reduction properties of Mb-MNP conjugates. The three types of Mb-MNP conjugates were adsorbed on HPG electrodes and tested for their ability to reduce *t*-BuOOH using rotating disk voltammetry. The current generated as the result of catalytic reduction of *t*-BuOOH to *t*-butanol by the films was measured as described previously.[8,35, 36] Fig. 11 depicts the representative voltammograms of the free Mb, free MNP, and Mb-MNPs films upon addition of 5 mM of *t*-BuOOH in anaerobic PBS solution. It is interesting to note that the onset reduction potentials of the catalytic voltammograms decreased with increasing amounts of MNPs in the Mb-MNP conjugates and were smaller than those of the free Mb and free MNPs films adsorbed on similar HPG electrodes (a to e in Fig. 11; data in Table 4).

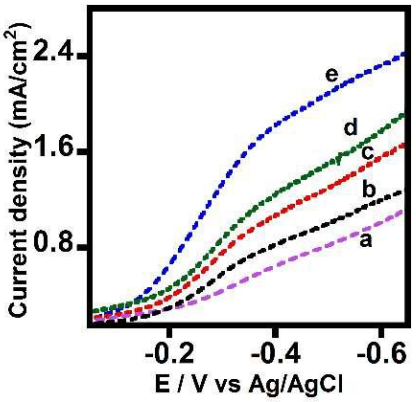

Fig. 11 Representative steady-state catalytic reduction voltammograms of *t*-BuOOH (5 mM), oxygen-free PBS, 25 ^{o}C catalyzed by: (a) free MNPs, (b) free Mb, (c) Mb-MNPs$_{1mg}$, (d) Mb-MNPs$_{5mg}$, and (e) Mb-MNPs$_{10mg}$ conjugates adsorbed on HPG electrodes, scan rate 0.3 Vs^{-1}, 1000 rpm electrode rotation rate.

Mb-MNPs$_{10mg}$ films on electrodes required the lowest onset peroxide reduction potential, suggesting that they had an energetically favored reduction process. In contrast, free Mb and free MNP films were catalytically active only at more negative onset potentials, suggesting a greater kinetic barrier for electron communication between the redox centers of Mb or MNPs and the electrode. Films of Mb-MNPs$_{1mg}$ and Mb-MNPs$_{5mg}$ displayed intermediate onset potentials. Thus, the influence of MNP amount used in the Mb-MNP conjugation in controlling the catalytic efficiency of the conjugates can be understood. The decrease in onset potentials with increase in MNP amount correlated with the corresponding increases in reduction currents observed (Fig. 11) and greater substrate affinity (Fig. 8D).

Table 4. Onset of peroxide reduction potentials.

Sample	Onset reduction potential vs. Ag/AgCl reference (mV)
a. MNP	–209 ± 13
b. Mb	–189 ± 11
c. Mb-MNPs$_{1mg}$	–166 ± 9
d. Mb-MNPs$_{5mg}$	–148 ± 10
e. Mb-MNPs$_{10mg}$	–131 ± 7

Conclusions

The results of this study demonstrate that by appropriately controlling the ratio of MNPs to enzyme catalysts, one can achieve cost-effective, economical, reusable, and stable bioreactors for green synthesis of fine chemicals and specialty materials. We additionally illustrated that a small amount of metalloprotein conjugated to MNPs could generate considerable amounts of product at a greater turnover rate when compared with a similar amount of free protein present in solution. The advantages of protein conjugation with MNPs include convenient preparation, efficient free protein recovery, effective reusability, easy product isolation, and long-term storage stability of protein-bound MNPs in comparison to the free protein solutions. Applicability to bioinspired organometallic catalysts in place of enzymes is one other related area of significance.

Acknowledgements

Research reported in this publication was supported, in part, by the National Institute of Diabetes and Digestive and Kidney Diseases of the National Institutes of Health (Award Number R15DK103386), and, in part, by the Oklahoma State University (Start-up and Technology Development funds). The content is solely the responsibility of the authors and does not necessarily represent the official views of the National Institutes of Health.

Notes and References

1. J. S. Beveridge, J. R. Stephens and M. E. Williams, *Annu. Rev. Anal. Chem*., 2011, **4**, 251-273.
2. J. Govan and Y. K. Gun'ko, *Nanomaterials*, 2014, **4**, 222-241.
3. T.-H.Shin, Y. Choi, S. Kim and J. Cheon, *Chem. Soc. Rev*., 2015, 10.1039/c4cs00345d.
4. R. Kaur, A. Hasan, N. Iqbal, S. Alam, M. K. Saini and S. K. Raza, *J. sep. sci*., 2014, **37**, 1805-1825.
5. L. H.Reddy, J. L. Arias, J. Nicolas and P. Couvreur, *Chem. Rev*., 2012, **112**, 5818-5878.
6. L. Gao, J. Zhuang, L. Nie, J. Zhang, Y. Zhang, N. Gu, T. Wang, J. Feng, D. Yang and S. Perrett, *Nat. Nanotech*., 2007, **2**, 577-583.
7. I. M. Obaidat, B. Issa and Y. Haik, *Nanomaterials*, 2015, **5**, 63-89.
8. S. Krishnan and C. Walgama, *Anal. Chem*., 2013, **85**, 11420−11426.
9. V. Singh and S. Krishnan, *Analyst*, 2014, **139**, 724 – 728.
10. A. R. Herdt, B.-S. Kim and T. A. Taton, Encapsulated magnetic nanoparticles as supports for proteins and recyclable biocatalysts, *Bioconjugate Chem*., 2007, **18**, 183-189.
11. M.-E. Aubin-Tam and K. Hamad-Schifferli, *Biomed. Mater*., 2008, **3**, 034001.
12. R. Hudson, Y. Feng, R. S. Varma and A. Moores, *Green Chem*., 2014, **16**, 4493-4505.
13. I. J. Bruce and T. Sen, *Langmuir*, 2005, **21**, 7029-7035.
14. Z. Ying, P. Siyi, W. Xuetuan, W. Lufeng and L. Yanlong, *BioResources*, 2013, **8**, 2605-2619.
15. L. Zhou, J. Wu, H. Zhang, Y. Kang, J. Guo, C. Zhang, J. Yuan and X. Xing, *J. Mater. Chem*., 2012, **22**, 6813-6818.
16 W. J. Goh, V. S. Makam, J. Hu, L. Kang, M. Zheng, S. L. Yoong, C. N. Udalagama and G. Pastorin, *Langmuir*, 2012, **28**, 16864-16873.
17. G. Zhao, J. Wang, Y. Li, X. Chen and Y. Liu, *J. Phys. Chem. C*., 2011, **115**, 6350-6359.
18. J. N. Talbert and J. M. Goddard, *Process Biochem*., 2013, **48**, 656-662.
19. D. Kelman, J. DeGray and R. Mason, J. Biol. Chem., 1994, **269**, 7458.
20. B. Munge, C. Estavillo, J. B. Schenkman and J. F. Rusling, *ChemBioChem*., 2003, **4**, 82-89.
21. E. N. Kadnikova and N. M. Kostic, *J. Mol. Catal. B: Enzym*., 2002, **18**, 39-48.
22. L. Su, W. Qin, H. Zhang, Z. U. Rahman, C. Ren, S. Ma and X. Chen, *Biosens. Bioelectron*., 2015, **63**, 384-391.
23. A.Tiraferri and M. Elimelech, *J. Memb. Sci.*, 2012**, 389**, 499-508.
24. S.-k. Kam and J. Gregory, *Colloids Surf., A: Physicochemical and Engineering Aspects*, 1999**, 159**, 165-179.
25. A. Nasti, N. M.Zaki, P. de Leonardis, S. Ungphaiboon, P. Sansongsak, M. G. Rimoli and N. Tirelli, *Pharm. Res.,* 2009, **26**, 1918-1930.
26 E. Illés and E. Tombácz, *J. Colloid Interface Sci.,* 2006, **295**, 115–123.
27. V. Singh and S. Krishnan, *Anal. Chem*., 2015, **87**, 2648-2654.
28. H. S. Choi, W. Liu, P. Misra, E. Tanaka, J. P. Zimmer, B. I. Ipe, M. G. Bawendi and J. V. Frangioni, *Nat. Biotechnol.*, 2007**, 25**, 1165-1170.
29. D. Hu, P. Zhang, P. Gong, S. Lian, Y. Lu, D. Gao and L. Cai, *Nanoscale.,* 2011**, 3**, 4724-4732.
30. H. Qu, D. Caruntu, H. Liu and C. J. O'Connor, *Langmuir*, 2011, **27**, 2271-2278.
31. Y. Goto and A. L. Fink, *J. Mol. Biol.,* **1990**, *214*, 803-805.
32. M. Fang, P. S. Grant, M. J. McShane, G. B. Sukhorukov, V. O. Golub and Y. M. Lvov, *Langmuir*, 2002, **18**, 6338-6344.
33 .E.-H. Lee, Y.-H. Lee and J.-C. Pyun, *Procedia Engineering*, 2012, **47**, 1023-1024.
34. R. Nerimetla and S. Krishnan, *Chem. Commun.,* 2015, **51**, 11681-11684.
35. P. M.Guto and J. F. Rusling, *J. Phys. Chem. B*., 2005, **109**, 24457-24464.
36. N. Li, J.-Z. Xu, H. Yao, J.-J. Zhu and H.-Y. Chen, *J. Phys. Chem. B*., 2006, **110**, 11561-11565.

TOC